## Auto-reverse nuclear migration in bipolar mammalian cells on micropatterned surfaces

B. Szabó <sup>1</sup>, Zs. Környei <sup>2</sup>, J. Zách <sup>3</sup>, D. Selmeczi <sup>3</sup>, G. Csúcs <sup>4</sup>, A. Czirók <sup>3</sup> and T. Vicsek <sup>1,3</sup>
February 5, 2008

Phone: +36 1 372 2795, Fax: +36 1 372 2757

**Running title:** Auto-reverse nuclear migration in mammalian cells.

**Keywords:** microtubule dynamics, centrosome, cell polarization, interkinetic nuclear migration, ventricular zone.

**Abbreviations:** AMP-PNP, 5'-adenylylimidodiphosphate; MLCK, myosin light-chain kinase; MT, microtubule; MTOC microtubule organizing center.

<sup>&</sup>lt;sup>1</sup> Research Group for Biological Physics, HAS, Budapest, Pázmány Péter sétány 1/A, 1117 Hungary.

<sup>&</sup>lt;sup>2</sup> Institute of Experimental Medicine, Budapest, Szigony u. 43, Hungary.

<sup>&</sup>lt;sup>3</sup> Department of Biological Physics, Eötvös University, Budapest, Pázmány Péter sétány 1/A, 1117 Hungary.

<sup>&</sup>lt;sup>4</sup> Laboratory for Biomechanics, ETH Zürich.

A novel assay based on micropatterning and time-lapse microscopy has been developed for the study of nuclear migration dynamics in cultured mammalian cells. When cultured on  $10\text{-}20~\mu\mathrm{m}$  wide adhesive stripes, the motility of C6 glioma and primary mouse fibroblast cells is diminished. Nevertheless, nuclei perform an unexpected auto-reverse motion: when a migrating nucleus approaches the leading edge, it decelerates, changes the direction of motion and accelerates to move toward the other end of the elongated cell. During this process cells show signs of polarization closely following the direction of nuclear movement. The observed nuclear movement requires a functioning microtubular system, as revealed by experiments disrupting the main cytoskeletal components with specific drugs. On the basis of our results we argue that auto-reverse nuclear migration is due to forces determined by the interplay of microtubule dynamics and the changing position of the microtubule organizing center as the nucleus reaches the leading edge. Our assay recapitulates specific features of nuclear migration (cell polarization, oscillatory nuclear movement), while allows the systematic study of a large number of individual cells. In particular, our experiments yielded the first direct evidence of reversive nuclear motion in mammalian cells, induced by attachment constraints.

Nuclear migration is an essential aspect of a number of cellular and developmental processes. Correct positioning of the nucleus within a eucaryotic cell can have various functions (Reinsch and Gönczy, 1998; Morris, 2000, 2003). For example, in budding yeast nuclear migration into the bud neck is required for correct segregation. In fission yeast a complex, oscillatory motion has been observed and interpreted with its relation to meiosis (Ding et al., 1998). Similar microtubule-dependent nuclear oscillations were reported in mutant budding yeast cells associated with a prolonged mitotic arrest (Thrower et al., 2003) In a number of non-vertebrate species the directed movements of the male and female pronuclei are also essential in zygote formation (Reinsch and Gönczy, 1998). Migration of nuclei to the cortex is the prerequisite for normal cellularization in the syntitial Drosophila embryo (Foe and Alberts, 1983).

Much less is known, however, about the role of and the mechanism by which the nucleus migrates in mammalian cells. The appropriate location of the nucleus can be relevant in several cell types: For instance, in the tightly packed pseudostratified epithelia nuclei of the elongated cells are arranged to avoid each other. In the pseudostratified ventricular epithelium of the developing and adult brain, nuclei of neuronal progenitor cells and radial glial cells oscillate between the ventricular and cortical surfaces (Nadarajah and Parnavelas, 2002; Alvarez-Buylla et al., 1998; Noctor et al., 2001). During this process, termed 'interkinetic nuclear migration', the position of the nucleus systematically depends upon the cell cycle phase and progenitor cells divide only at the ventricular surface. Although the mechanism of this remarkable phenomenon is still not clear (Murciano et al., 2002; Frade, 2002); maintaining a strongly polarized, elongated morhoplogy seems to be associated with the consistent work of the apparatus responsible for moving the nucleus (Fukushima et al., 2000).

Chemically micropatterned surfaces offer a nice and elegant way to manipulate cell shape and to a certain extent also cell function (Singhvi et al., 1994; Chen et al., 1997, 1998; Craighead et al., 2001). We have also shown previously that a method based on microcontact printing is well suited to manipulate cell-shape in a controlled way (Csúcs et al., 2003). In order to combine the advantages of time-lapse microscopy, the potential of *in vitro* manipulations and the necessary condition of the cell's bipolarity we designed an *in vitro nuclear migration assay* made of micropatterned 10 to 20 micron wide, cell adhesive stripes separated from each other by attachment restricting stripes. The effects of such a confined geometry are twofold: cells assume an elongated morphology, while their locomotion is inhibited. As a result, we have a device in which motion of the nuclei can be followed in great detail over a long period of time. In turn, this enables us to characterize the nuclear motion both qualitatively and quantitatively. Our main observation is that cells under such conditions often exhibit a puzzling oscillatory motion of the nucleus. This process is seen in various mammalian cell cultures and characterized by continuous deceleration, change in the direction of motion and acceleration to move towards the other end of the elongated cell.

The questions we address in this work are concerned with the biophysical (forces, dynamics) and the cell biological (cytoskeletal proteins involved) background of this reversive nuclear migration. One motivation for this is the appreciation of the fact that in addition to being a tiny biochemical factory, our cells contain a number of microscopic machines performing mechanical work. With great advances in nanotechnology, there is an increasing potential and need in the quantitative understanding of this essential – forces versus motion – aspect of the cellular machinery.

Cell Cultures. Cultures of C6, U87 gliomas, and 3T3 fibroblast cell lines were grown in Minimum Essential Medium (MEM; Sigma) supplemented with 10% fetal calf serum (FCS; Gibco), 4 mM glutamine and 40  $\mu$ g/ml gentamycin in humidified air atmosphere containing 5% CO<sub>2</sub>, at 37 °C. Primary fibroblasts were isolated from the bodies of 13 day old mouse embryos and were grown to confluency in DMEM (Sigma) containing 10% FCS. Prior to the time-lapse experiments cells were passaged over the micropatterned surfaces of 35 mm plastic petri dishes (Greiner) at a density of  $1 - 1.5 \cdot 10^4$  cell/cm<sup>2</sup>. In some experiments the stripe pattern was printed on a 25 mm glass coverslip, which was then placed into a petri dish.

**Microscopy.** Time-lapse recordings were performed on a computer-controlled Leica DM IRB inverted microscope equipped with 10x, 20x objectives and an Olympus Camedia 4040z digital camera. Cell cultures were kept at 37 °C in humidified 5% CO<sub>2</sub> atmosphere within a custom-made incubator attached to the microscope stage (Hegedűs et al., 2000; Czirók et al., 2002). Phase contrast images were acquired in every 5 min for 2-3 days.

**Micropatterning.** Chemically structured substrates containing 10-20  $\mu$ m wide stripes permitting and restricting cell attachment were prepared by microcontact printing. Adhesive surfaces were coated with either 40  $\mu$ g/ml fibronectin with 20  $\mu$ g/ml Alexa488-labeled fibrinogen (Molecular Probes), or 50  $\mu$ g/ml FITC-labeled poly-1-lysine (SIGMA). Blocking of protein/cell attachment was achieved by a subsequent covering the surfaces with poly-1-lysine-g-poly(ethylene glycol) (PLL-PEG) (Huang et al., 2001). For further details see (Csúcs et al., 2003).

**Drugs.** Specific drugs (SIGMA) were used to affect various cytoskeletal proteins. Microtubule (MT) disruption was induced by 20-100 nM vinblastine, MT dynamics was shifted towards polymerization by 10-100 nM taxol (Blagosklonny and Fojo, 1999; Grigoriev et al., 1999). Cytoplasmic dyneins were inhibited by 5 μM sodium-orthovanadate (Murray et al., 2000), kinesins by 100  $\mu$ M 5'-adenylylimidodiphosphate (AMP-PNP) (Holzinger and Lutz-Meindl, 2002). F-actin was influenced by 100-500 nM cytochalasin-D (Wakatsuki et al., 2001). Myosin-II activity was inhibited by the myosin light-chain kinase (MLCK) inhibitor ML-7 at concentrations of 1 and 10  $\mu$ M (Bain et al., 2003). Reagents were added to the culture medium after one day long time-lapse recording in normal medium. Drug effectiveness was tested by standard viability assays (Mosmann, 1983). Briefly, C6 cells treated for 24 hour with various concentrations of drugs were incubated with 3-(4,5-dimethylthiazol-2-yl)-2,5-diphenyltetrazolium bromide (MTT, 25 mg/ml). 2 hours later cells and formazan crystals were dissolved in acidic (0.08 M HCl) isopropanol and transferred onto 96 well plates. Optical density (OD) was determined at a measuring wavelenght of 570 nm against 630 nm as reference using an SLT 210 ELISA-reader. We administered the drugs in non-toxic concentrations in the time-lapse experiments. The use of vanadate in cell culture is not straightforward because the permeability of the cell membrane to vanadate can be problematic. We used vanadate in a concentration of 5  $\mu$ M, as a dose, which still resulted in a reduction of overall cell viability. Time-lapse recordings did not show alterations in the rate of cell decay, cellular morphology or in the nuclear motility of cells upon treatment with 5  $\mu$ M vanadate.

**Immunocytochemistry.** Cells grown on micropatterned glass coverslips were fixed immediately following the termination of the time-lapse recording (4% paraformaldehyde in PBS for 20 min at room temperature). Membranes of fixed cells were permeabilized by treatment with Triton X-100 (5 min, 0,1% v/v in PBS). Non-specific antibody binding was

Praha) and  $\gamma$ -tubulin (rabbit; Sigma) were used at dilutions of 1 to 1000-5000, respectively. Secondary antibodies to  $\alpha$ -tubulin were Cy3 (1:3000, Jackson) or Alexa488 labeled anti-mouse IgG-s (1:1000, Molecular Probes).  $\gamma$ -tubulin was visualised by 1.5 hour incubation with biotin-conjugated anti-rabbit IgG (1:1000, Vector) followed by 1 hour incubation with fluorescent avidin-TRITC (1:750, Sigma). The immunolabeled sample was compared to the last frame of the obtained recording. By locating the same cells in both images, we were able to identify the relationship between nuclear motion and the distribution of labeled protein complexes. Thus, each immunostained frame contained an assembly of cells with nuclei stopped at various stages of their motion.

Data processing and analysis. Cell nucleus positions together with the two process ends were determined manually in each time-lapse frame using a custom-written software. The procedure resulted in the nucleus position data  $x_i(t)$ , which denotes the location of the nucleus of cell i along the stripe at a time point t. The duration of each nuclear migration period was determined as the elapsed time between the peaks of  $x_i(t)$ . Velocity of the nucleus was calculated from its net displacement in a 30 minute-long time interval as  $v_i(t) = [x_i(t+\tau/2) - x_i(t-\tau/2)]/\tau$ , where  $\tau = 30$ min. The nuclear migration activity during a time period T was characterized by the average magnitude of nuclear velocities as  $V_T = \langle |v_i(t)|\rangle_{i,t\in T}$ , where the average  $\langle \rangle_{i,t\in T}$  is calculated over all nuclei i which were oscillating within the time period T. Drug effects were characterized by comparing nuclear migration activity of the first day (control) to that of the second day (drug exposed) as  $V_{D2}/V_{D1}$ . To establish the statistical significance of the differences, velocity data was sampled at 1h intervals. The resulting velocity magnitudes (absolute values), characterizing the cell population before and after the drug exposure, were compared by two-sample t-tests.

Online supplemental material. Video 1 displays the motility of C6 cells on the surface of 20  $\mu$ m wide Alexa488-labeled fibronectin-fibrinogen stripes. Video 2 shows the reversive nuclear motion in a single C6 cell on a similar stripe. Frame size:  $270x60 \ \mu\text{m}^2$ . Video 3 (frame size:  $400x115 \ \mu\text{m}^2$ ), 4 (frame size:  $250x50 \ \mu\text{m}^2$ ), and 5 (frame size:  $630x480 \ \mu\text{m}^2$ ) show the effect of 30 nM taxol (administered at 16 h), 20 nM vinblastine (administered at 9 h), and 500 nM cytochalasin D (administered at 12 h) respectively on auto-reverse nuclear migration in C6 cells cultured on 20  $\mu$ m wide stripes.

**Nuclear migration assay on micropatterned surfaces.** Various cell types were cultured on micropatterned substrates, consisting of alternating stripes permitting (fibronectin-fibrinogen or poly-l-lysine) and restricting (PLL-PEG) cell attachment. As Fig. 1 demonstrates, under these conditions cells assume a highly elongated, bipolar morphology. Cell cultures, grown on the micropatterned substrates, were recorded for two days with computer controlled microscopy. The recordings show that while net cell movements diminish, locomotory activity remains present: Both processes of the bipolar cells still exhibit – intermittently – a leading edge-like dynamics with membrane ruffling and filopodium activity (Video 1).

Surprisingly, cell nuclei often engage in an oscillatory movement. As shown in Fig. 2, when a migrating nucleus approaches one of the leading edges, it reverses direction and continues to move in the opposite direction without a lag period (Video 2). During direction reversals the nuclei do not rotate, but retain orientation (data not shown). Nuclei were often observed to perform multiple (up to 15) such cycles between cell divisions. The reversive nuclear motion is attachment constraint specific. It was exhibited in  $32 \pm 7\%$  of C6 cells when cultured on  $20 \mu m$  wide stripes (data from 4 independent cultures). In non-micropatterned control cultures nuclear oscillation was found solely in elongated cells, never in flattened cells. Characteristic width of bipolar C6 cells is between 10 and  $20 \mu m$ , which implies that on  $20 \mu m$  or wider stripes bipolar cells do not respond to the full line width. They still show reversive nuclear motion.

**Cell polarization.** Cells with a migrating nucleus also show signs of polarization. Usually the front edge, toward which the nucleus moves, exhibits more membrane ruffling activity. At the same time the trailing edge narrows and occasionally detaches (Fig. 2). This polarization reverses together with the directionality of nuclear motion. Sister cell nuclei tend to oscillate with opposite polarization after mitosis, especially on the very narrow (10  $\mu$ m) stripes (Fig. 3).

Reversive nuclear motion in various cell types. The extent of attachment constraint-induced nuclear oscillation is cell type specific. We found the phenomenon most prominently in C6 cells, where the average period length of the oscillation was  $4.6 \pm 0.4$  h (Fig. 4a). In primary fibroblast cells the nucleus reverses direction further from the leading edges, reducing thereby their average period length to  $1.8 \pm 0.25$  h (Fig. 4b). 3T3 nuclei are also motile, but usually fail to reverse direction. Finally, U87 cells exhibit a less elongated morphology and display less pronounced nuclear motility. A substantial variability was found among individual cells even within the same culture. The population standard deviation of period lengths is approximately 40%, i.e., 1.9 h and 0.6 h for C6 cells and primary fibroblasts, respectively.

**Temporal resolution of nuclear motion.** To better characterize the dynamics of reversive nuclear motion, cell nuclei and process ends were tracked on consecutive images. The resulting position data (Fig. 5) demonstrate that reversals in nuclear motion direction are coupled to the destabilization and partial detachment of the new trailing processes. Velocities, calculated from changes in nuclear positions, show that nuclei slow down, reverse direction and then accelerate in a smooth, continuous manner. Thus, the temporal changes in positions and velocities give no evidence for that the gradual deceleration and reversing direction could be attributed to distinct mechanisms.

Despite the differences in period lengths, the average speed (i.e., the average absolute value of the velocity) of the nuclei was found to be similar in both C6 ( $29 \pm 13 \mu \text{m/h}$ ) and primary fibroblast ( $26 \pm 10 \mu \text{m/h}$ ) cells. To extract the typical velocity of active nuclear movement, in each oscillatory period we determined its maximal speed. The distribution of these maximal velocities (Fig. 6) shows a peak around  $50\mu \text{m/h}$ . However, several nuclei were also observed moving faster than  $100 \mu \text{m/h}$ .

constraint-induced nuclear motion, further experiments were carried out with C6 cells in our micropatterned assay. Population-averaged nuclear speeds were calculated as a quantitative measure of nuclear motion activity. The major force generating cytoskeletal elements were targeted with specific drugs: cytochalasin D (actin polymerization inhibitor), vinblastine (MT destabilizing agent), taxol (MT stabilizator), ML-7 (myosin-II MLCK inhibitor), vanadate (dynein inhibitor) and AMP-PNP (as kinesin inhibitor with low specificity).

Nuclear motion was strongly attenuated by both drugs that disrupt MT dynamics (Table 1, Fig. 7, Video 3 and Video 4). Taxol and vinblastine effectively blocked the motion of the nuclei above 10 nM and 20nM concentrations, respectively. These two drugs, however, have an opposite effect on cell morphology: while vinblastine reduces, taxol increases the elongation of the cell shape. After the administration of taxol, several cells could divide, which confirms the mildness of the intervention. Effect of vinblastine was more massive: cells stopped nuclear migration abruptly. Although cells lost their long processes, they remained bipolar, which suggests a moderate disassembly of microtubules.

Drugs affecting the actin cytoskeleton and the actin-myosin system altered nuclear motion only when administered at very high (above specific) concentrations. In particular, 500 nM cytochalasin D reduced nuclear motion without changing the cell shape (Video 5), at lower concentrations it was ineffective. Kinesin and cytoplasmic dynein inhibitors had no effect on nuclear motility. Finally, the replacement of the fibronectin-fibrinogen substrate to poly-1-lysine did not alter nuclear motion, either.

MTOC position is correlated with the direction of nuclear motion. At the end of time-lapse recordings the cultures were fixed for anti- $\alpha$  tubulin and anti- $\gamma$  tubulin immunolabeling. C6 cells, in which the nucleus was moving just prior the fixation, were selected from the time-lapse recordings. Subsequently, microtubules and MT organizing centers (MTOC) were visualized in these cells by epifluorescence and confocal microscopy. The MTOC was always located either behind or beside the nucleus, between the plasma and nuclear membranes, i.e., MTOC positions segregated into two groups, one group at the back, another group at the mid-point of the nucleus (Fig. 8). Generally, MTOC was positioned at the back of the nucleus, when the cell was fixed soon after the nucleus reversed its direction, and in cells with a nucleus at the mid-point moved faster. Nuclei were not moving in cells exhibiting two opposite MTOCs, each facing a different cell process. The anti- $\alpha$  tubulin immunostaining revealed densely packed microtubules, mainly parallel to the cell axis (image not shown).

**Nuclear motion is needed for proper development.** Active repositioning of the nucleus is an integral part of various cell biological processes including locomotion and division (Bray, 2000). Most of the *in vivo* occuring cases of nuclear motility has important developmental aspects including fertilization, zygote formation, cellularization and spatially and temporally regulated cell production. The most relevant example of oscillatory nuclear movement, interkinetic nuclear migration, seems to be essential in the proper timing and abundancy of neuron formation: The normal course of interkinetic nuclear migration can be blocked by a defective function of the human LIS1 gene. In such cases a severe disease, lissencephaly, develops which results in mental retardation, epilepsy and usually death at an early age (Dobyns and Truwit, 1995; Morris, 2000).

Nuclear migration assay. Capitalizing on the promising potential of micropatterned surfaces in biomedical engineering (Zhang et al., 1999; Folch and Toner, 2000), we developed an assay where cell shape and migratory activity can be systematically controlled (Brock et al., 2003). In particular, the narrow stripes of attachment-permitting surfaces effectively inhibited cellular locomotion, presumably as a result of hindered lamellipod formation. This suppression of locomotion helped us to uncouple the motion of the nucleus from that of the whole cell. Nevertheless cellular polarization, which we determined on the bases of MTOC position as well as membrane ruffling distribution along the cell perimeter, remained present. The resulting assay thus recapitulates most features of nuclear migration (cell polarization, reversive nuclear movement), while allows the systematic study of a large number of individual cells. Our experiments yielded the first direct evidence of attachment constraint-induced reversive nuclear motion in vertebrate cells.

Nuclear positioning is MT-dependent. Nuclear migration was blocked by low concentrations of vinblastine or taxol. These drugs are tubulin-specific, either depolymerizing or stabilizing MTs and thus inhibiting their normal dynamics. Therefore, a functioning MT system is essential for nuclear migration in our essay. This finding is in concert with results of recent studies performed in a variety of experimental systems, which clearly indicated the fundamental role of microtubules in nuclear positioning (Morris, 2000, 2003). The critical role of a perinuclear microtubule fork in nuclear translocation has been revealed in neurons (Xie et al., 2003). In vitro experiments with purified proteins demonstrated that microtubule polymerization alone is capable of pushing MTOC-like structures into the geometrical center of microfabricated chambers (Holly et al., 1997; Faivre-Moskalenko and Dogterom, 2002). The force generated by tubulin polymerization can be in the order of a few pN – similar to that of exerted by molecular motors (Dogterom and Yurke, 1997). MT polymerization and physical pushing of the nucleus was demonstrated to contribute to nuclear positioning in fission yeast (Tran et al., 2001).

In animal cells, gene products that affect MT stability like Lis1 (Sapir et al., 1997) and CLASP (Akhmanova et al., 2001) were uniquely found on MT plus ends. The role of Lis1 in nucleokinesis was directly demonstrated by altered migratory behavior of cerebellar granule cells explanted from a Lis1 knockout mouse (Hirotsune et al., 1998). A number of other proteins like dynactin and CLIP (Vaughan et al., 1999), which are known to be involved in nuclear positioning of mammalian cells, also specifically localize on MT plus ends. Nevertheless, the functional role of these proteins, as well as the operational integration of this multi-component process remains unclear. Experiments using vanadate and the ATP analogue AMP-PNP as inhibitory agents yielded negative results, which suggests that within our assay cytoplasmic dyneins and kinesins do not have a central role in nuclear migration. F-actin disruption by cytochalasin D and myosin-II inhibition by the MLCK inhibitor ML-7 shows that nuclear migration is not sensitively actin- or myosin-dependent, either.

found that cell polarization strongly correlated with the direction of nuclear movement. The MTOC was always located either behind or beside the nucleus, which reinforces a more complex relationship between MTOC position and the direction of cell movement than the general assumption that MTOC leads the way (Schütze et al., 1991; Schliwa and Höner, 1993; Ueda et al., 1997; Yvon et al., 2002). Moreover, the change in nuclear movement direction involved an immediate destabilization and partial collapse of the former leading edge. Further experiments may reveal the molecular connection between the change in cell polarization and the gradually decreasing nuclear velocity at the reversing points.

Cell cycle. The most prominent connection between cell cycle and oscillatory nuclear movement is exhibited in the interkinetic nuclear migration of avian and mammalian neural stem cells (Takahashi et al., 1996). In this case the cell cycle and the nuclear oscillation is so strongly coupled, that typically there is a single oscillation in each cell cycle. In fission yeast, oscillatory nuclear motion was also observed during the prophase of meiosis (Ding et al., 1998). In that case the cell shape was also strongly elongated, however, the period of the motion was much shorter (ca. 10 minutes) than the duration of the cell cycle (and even that of the prophase), allowing multiple nuclear oscillations per cell cycle. In our assay the period of the reversive nuclear motility was substantially longer, in the range of 2-5 h. This period is still much shorter than the typical cell cycle length, approximately a day. Moreover, nuclear oscillations could be observed practically during the entire cell cycle, not just prior mitosis. Therefore, in our assay we have no evidence for a strong coupling between cell cycle phases and nuclear positioning.

Forces involved in nuclear migration. Forces associated with moving the nucleus in a viscous medium can be estimated from the following considerations (Dogterom and Yurke, 1998). Cell plasma is not a homogeneous liquid as fibrous elements of the cytoskeleton have a significant impact on the drag sensed by the nucleus. Nevertheless, based on the Stokes formula, an effective viscosity value  $\eta$  can be obtained from simultaneous measurements of the force F acting on an intracellular passive test particle, its size r and velocity v, as  $F=6\pi\eta rv$ . Such measurements resulted in  $\eta\approx 100$  Pas (Bausch et al., 1999; Caspi et al., 2002). Applying this result to the nucleus ( $\mathbf{r}=5\mu\mathrm{m}$ ,  $v\approx 50\mu\mathrm{m/h}$ ) yields  $F\approx 100pN$  for the driving force. We regard this value as an upper estimate, as it is highly likely that cytoskeletal components are disassembled in front of the moving nucleus, thus the apparent viscosity is less than that in the case of an inert test object. Although currently it is impossible to estimate the significance of cytoskeletal disassembly, we expect the driving force to be  $F\approx 10pN$ . As 1 pN is the typical yield of molecular force generating mechanisms (molecular motors, tubulin polymerization, etc.), the nuclear motile force could be resulted by already a handful of molecular complexes.

**Model for nucleokinesis.** Based on our experiments we suggest that the force, which drives nuclear migration in elongated cells, is MT-dependent, and originates from MT polymerization. At the observed nuclear migration speeds, the force a single polymerizing MT can exert is  $\sim$  1pN (Dogterom and Yurke, 1997), thus in the proposed model a few dozen MTs are expected to push the nucleus. For a steady, unidirectional motion the underlying left-right symmetry of the system has to be broken. Usually this is realized by molecular concentration gradients, or as in case of molecular motors, by the molecular polarity of the substrate.

In our case a plausible explanation for the origin of symmetry breaking is provided by the enforced narrow shape of the cell. In this configuration the microtubules emanating from the MTOC can preferably grow only in one direction (Fig. 9). As a result, the reactive force of their polymerization due to dynamic instability propels the MTOC together with

the force continues to act upon the MTOC and makes its former location behind the nucleus unstable. As the MTOC is pushed "over" the nucleus, gradually the MTOC-attached MTs are destabilizing while new ones are growing towards the closer cell edge, resulting in a new, backward-directed propulsive force.

The asymmetry needed for directional nuclear movement could also be generated by different MT polymerization rates at the front and rear cell process. The rate difference could be resulted by the presence of a molecular gradient, strongly coupled to cell polarization and motility. Such a gradient is exhibited, e.g., by the rho family GTPases, which are considered as constituents of a master controller of directional cell motility(Wittmann and Waterman-Storer, 2001) and their downstream targets like PKC $\zeta$  (Etienne-Manneville and Hall, 2003). In this framework, a feedback is predicted which makes the maintenance of the gradient incompatible with certain nuclear positions. The conjectured feedback may involve the interaction of nuclear membrane-localized proteins with cdc42 or its downstream targets.

C6 glioma cells, where reversive nuclear motion was most prominently exhibited, share many properties with the radial glial cells, which were found to be neural stem cells (Friedlander et al., 1998; Campbell and Gotz, 2002). It has also been shown recently that microtubules, but not microfilaments, are critical for the polarized morphology of the C6 cells (Li et al., 2003). However, as reversive nuclear motion was not restricted to glia-derived cells, we presume the phenomenon is the result of a general cell biological mechanism, present in various cell types. Although the clarification of this point needs further studies, we predict that the elongated cell shape and an asymmetrically localized MTOC should lead to the directed motion of the attached nucleus in most cell types.

The authors are most grateful to János Kovács and Balázs Hegedűs for their help in implementing the micropatterned technology. We thank Zsófia Jurányi, Gergely Nagy and Rita Vass for their valuable help in evaluating the time-lapse recordings. The useful comments of profs. János Kovács and Dennis Bray are greatly appreciated. The mouse primary fibroblasts were kindly provided by Károly Markó. We thank Emilia Madarász for providing the conditions for cell culturing and immunocytochemistry. This research was supported by Hungarian Science Research Funds, OTKA T034995 and F038110, and NKFP 3A/0005/2002.

- Akhmanova A, Hoogenraad C, Drabek K, Stepanova T, Dortland B, Verkerk T, Vermeulen W, Burgering B, De Zeeuw C, Grosveld F, Galjart N. 2001. Clasps are clip-115 and -170 associating proteins involved in the regional regulation of microtubule dynamics in motile fibroblasts. Cell 104:923–935.
- Alvarez-Buylla A, Garcia-Verdugo JM, Mateo AS, Merchant-Larios H. 1998. Primary neural precursors and intermitotic nuclear migration in the ventricular zone of adult canaries. J Neurosci 18:1020–37.
- Bain J, McLauchlan H, Elliott M, Cohen P. 2003. The specificities of protein kinase inhibitors: an update. Biochem J 371:199–204.
- Bausch AR, Moller W, Sackmann E. 1999. Measurement of local viscoelasticity and forces in living cells by magnetic tweezers. Biophys J 76:573–79.
- Blagosklonny MV, Fojo T. 1999. Molecular effects of paclitaxel: myths and reality (a critical review). Int J Cancer 83:151–56.
- Bray D. 2000. Cell Movements. New York: Garland, 2nd ed.
- Brock A, Chang E, Ho CC, Leduc P, Jiang X, Whitesides GM, Ingber DE. 2003. Geometric determinants of directional cell motility revealed using microcontact printing. Langmuir 19:1611–17.
- Campbell K, Gotz M. 2002. Radial glia: multi-purpose cells for vertebrate brain development. Trends Neurosci 25:235–38.
- Caspi A, Granek R, Elbaum M. 2002. Diffusion and directed motion in cellular transport. Phys Rev E 66:011916.
- Chen CS, Mrksich M, Huang S, M. G, Whitesides, Ingber DE. 1997. Geometric control of cell life and death. Science 276:1425–28.
- Chen CS, Mrksich M, Huang S, Whitesides GM, Ingber DE. 1998. Micropatterned surfaces for control of cell shape, position, and function. Biotechnol Prog 14:356–63.
- Craighead HG, James CD, Turner AMP. 2001. Chemical and topographical patterning for directed cell attachment. Current Opinion in Solid State Materials Science 5:177–84.
- Csúcs G, Michel GR, Lussi JW, Textor M, Danuser G. 2003. Microcontact printing of novel co-polymers in combination with proteins for cell-biological applications. Biomaterials 24:1713–20.
- Czirók A, Rupp P, Rongish B, Little C. 2002. Multi-field 3D scanning light microscopy of early embryogenesis. J Microsc 206:209–17.
- Ding DQ, Chikashige Y, Haraguchi T, Hiraoka Y. 1998. Oscillatory nuclear movement in fission yeast meiotic prophase is driven by astral microtubules, as revealed by continuous observation of chromosomes and microtubules in living cells. J Cell Sci 111:701–712.
- Dobyns W, Truwit C. 1995. Lissencephaly and other malformations of cortical development: 1995 update. Neuropediatrics 26:132–47.

- Dogterom M, Yurke B. 1998. Microtubule dynamics and the positioning of microtubule organizing centers. Phys Rev Lett 81:485–88.
- Etienne-Manneville S, Hall A. 2003. Cell polarity: Par6, apkc and cytoskeletal crosstalk. Curr Opin Cell Biol 15:67–72.
- Faivre-Moskalenko C, Dogterom M. 2002. Dynamics of microtubule asters in microfabricated chambers: The role of catastrophes. PNAS 99:16788–19793.
- Folch A, Toner M. 2000. Microengineering of cellular interactions. Annu Rev Biomed Eng 02:227-56.
- Frade J. 2002. Interkinetic nuclear movement in the vertebrate neuroepithelium: encounters with an old acquaintance. Prog Brain Res 136:67–71.
- Friedlander DR, Brittis PA, Sakurai T, Shif B, Wirchansky W, Fishell G, Grumet M. 1998. Generation of a radial-like glial cell line. J Neurobiol 37:291–304.
- Fukushima N, Weiner J, Chun J. 2000. Lysophosphatidic acid (LPA) is a novel extracellular regulator of cortical neuroblast morphology. Dev Biol 228:6–18.
- Grigoriev IS, Chernobelskaya AA, Vorobjev IA. 1999. Nocodazole, vinblastine and taxol at low concentrations affect fibroblast locomotion and saltatory movements of organelles. Membr Cell Biol 13:23–48.
- Hegedűs B, Czirók A, Fazekas I, Bábel T, Madarász E, Vicsek T. 2000. Locomotion and proliferation of glioblastoma cells in vitro: statistical evaluation of videomicroscopic observations. J Neurosurg 92:428–434.
- Hirotsune S, Fleck M, Gambello M, Bix G, Chen A, Clark G, Ledbetter D, McBain C, Wynshaw-Boris A. 1998. Graded reduction of Pafah1b1 (Lis1) activity results in neuronal migration defects and early embryonic lethality. Nat Genet 19:333–339.
- Holly TE, Dogterom M, Yurke B, Leibler S. 1997. Assembly and positioning of microtubule asters in microfabricated chambers. PNAS 96:6228–31.
- Holzinger A, Lutz-Meindl U. 2002. Kinesin-like proteins are involved in postmitotic nuclear migration of the unicellular green alga micrasterias denticulata. Cell Biol Int 26:689–97.
- Huang NP, Michel R, Vörös J, Textor M, Hofer R, Rossi A, Elbert DL, Hubbell JA, Spencer ND. 2001. Poly(l-lysine)-g-poly(ethylene glycol) layers on metal oxide surfaces: Surface-analytical characterization and resistance to serum and fibrinogen adsorption. Langmuir 17:489–98.
- Li H, Berlin Y, Hart R, Grumet M. 2003. Microtubules are critical for radial glial morphology: Possible regulation by MAPs and MARKs. Glia 44:37–46.
- Morris NR. 2000. Nuclear migration: from fungi to the mammalian brain. J Cell Biol 148:1097–1101.
- Morris NR. 2003. Nuclear positioning: the means is at the ends. Curr Opin Cell Biol 15:54-59.
- Mosmann T. 1983. Rapid colorimetric assay for cellular growth and survival: application to proliferation and cytotoxicity assays. J Immunol Methods 65:55–63.

- the regulation of neurogenesis. Mol and Cell Neuroscience 21:285–300.
- Murray JW, Bananis E, Wolkoff AW. 2000. Reconstitution of atp-dependent movement of endocytic vesicles along microtubules in vitro: an oscillatory bidirectional process. Mol Biol Cell 11:419–33.
- Nadarajah B, Parnavelas JG. 2002. Modes of neuronal migration in the developing cerebral cortex. Nature Reviews Neuroscience 3:423–32.
- Noctor S, Flint A, Weissman T, Dammerman R, Kriegstein A. 2001. Neurons derived from radial glial cells establish radial units in neocortex. Nature 409:714–20.
- Reinsch S, Gönczy P. 1998. Mechanisms of nuclear positioning. J Cell Sci 111:2283–95.
- Sapir T, Elbaum M, Reiner O. 1997. Reduction of microtubule catastrophe events by LIS1, platelet-activating factor acetylhydrolase subunit. EMBO J 16:6977–6984.
- Schliwa M, Höner B. 1993. Microtubules, centrosomes and intermediate filaments in directed cell movement. Trends in Cell Biol 3:377–80.
- Schütze K, Maniotis A, Schliwa M. 1991. The position of the microtubule-organizing center in directionally migrating fibroblasts depends on the nature of the substratum. PNAS 88:8367–71.
- Singhvi R, Kumar A, Lopez G, Stephanopoulos GN, Wang DIC, Whitesides GM, Ingber DE. 1994. Engineering cell-shape and function. Science 264:696–98.
- Takahashi T, Nowakowski R, Caviness V. 1996. Interkinetic and migratory behavior of a cohort of neocortical neurons arising in the early embryonic murine cerebral wall. J Neurosci 16:5762–76.
- Thrower DA, Stemple J, Yeh E, Bloom K. 2003. Nuclear oscillations and nuclear filament formation accompany single-strand annealing repair of a dicentric chromosome in saccharomyces cerevisiae. Journal of Cell Science 116:561–69.
- Tran PT, Marsh L, Doye V, Inoue S, Chang F. 2001. A mechanism for nuclear positioning in fission yeast based on microtubule pushing. J Cell Biol 153:397–411.
- Ueda M, Gräf R, MacWilliams HK, Schliwa M, Euteneuer U. 1997. Centrosome positioning and directionality of cell movements. PNAS 94:9674–78.
- Vaughan K, Tynan S, Faulkner N, Echeverri C, Vallee R. 1999. Colocalization of cytoplasmic dynein with dynactin and clip-170 at microtubule distal ends. J Cell Sci 112:1437–1447.
- Wakatsuki T, Schwab B, Thompson NC, Elson EL. 2001. Effects of cytochalasin d and latrunculin b on mechanical properties of cells. J Cell Sci 14:1025–36.
- Wittmann T, Waterman-Storer C. 2001. Cell motility: can rho GTPases and microtubules point the way? J Cell Sci 114:3795–3803.
- Xie Z, Sanada K, Samuels BA, Shih H, Tsai LH. 2003. Serine 732 phosphorylation of fak by cdk5 is important for microtubule organization, nuclear movement, and neuronal migration. Cell 114:469–82.

wound-edge cells is cell type specific. Mol Biol Cell 13:1871–80.

Zhang S, Yan L, Altman M, Lassle M, Nugent H, Frankel F, Lauffenburger D, Whitesides G, Rich A. 1999. Biological surface engineering: a simple system for cell pattern formation. Biomaterials 20:1213–1220.

epifluorescence from 20  $\mu$ m wide FITC-poly-l-lysine stripes (green). Due to the constrained cell attachments, cells assume elongated, bipolar morphology. The positions of cell nuclei (arrowheads) are clearly recognizable. (Corresponding

supplemental material: Video 1.)

Figure 2: Attachment constraint-induced reversive nuclear motion. A well-spread C6 cell (left panel) shows no nuclear

displacements. The same cell type on the same substrate display reversive nuclear movement, when forced into a polarized

morphology by seeding onto a micropatterned substrate (middle panel). Similar behavior is seen in primary fibroblast

cultures (right panel), where the period of oscillation is decreased compared to that of C6 cells. Images were taken 1h

and 10 min apart for the C6 and the fibroblast cell, respectively. Scale bars: 50  $\mu$ m. (Supplement showing the reversive

nuclear motion of a C6 cell: Video 2.)

Figure 3: Nuclear motion after cell divison. The reversive nuclear motion starts immediatelly after the reattachment of

daughter cells, when the two nuclei begin to move in opposite directions. The semi-synchronous cells do not seem to keep

a continuous physical contact: cell-cell connections may break when the nuclei are at distal positions. Scale bar:  $100 \mu m$ .

Figure 4: Nuclear oscillation period lengths in C6 (a) and primary fibroblast (b) cells.

Figure 5: Dynamics of reversive nuclear motion. For selected cells the nucleus and the ends of both cell process were

followed frame-by-frame. The resulting positions – along the stripes – are plotted versus the time elapsed after seeding

in panel (a). The calculated corresponding nuclear velocities are shown in panel (b). During the 20h long time period,

the traced nucleus completed 4 full oscillations. The gradually increasing cell length reflects cell reattachment after a

division. After each direction reversal, the former leading edge partially detaches (arrowheads). The direction reversal of

the nucleus occurs within a process which changes the nuclear velocity in an almost linear fashion. The dotted lines mark

the time moments, when the nucleus moves with a maximal speed.

Figure 6: The distribution of the maximal velocities within each period reveals that the typical speed of active nuclear

movement is around 50  $\mu$ m/h.

Figure 7: Cytoskeleton affecting drugs can inhibit nuclear migration in C6 cells. The effects of drugs were characterized

by the relative change in average nuclear speeds before and after the administration of the drug. Error bars represent

standard deviation. Both vinblastine and taxol had a robust inhibitory effect (p $< 10^{-4}$ ), while the rest of the drugs did not

result in a significant alteration of nuclear motion (p> 0.1).

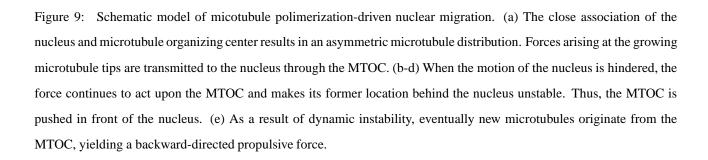
Figure 8: Correlation between MTOC position and nuclear migration direction. MTOC position was determined by  $\gamma$ -

tubulin immunostaining of the specimen, fixed immediatelly after the recordings (panel a). The obtained MTOC positions

are summarized in a shematic diagram (panel b). The arrow indicates the direction of motion. Cells had either one (full

circles) or two (crosses) MTOCs. When the investigated nucleus was moving, the attached MTOC was never found in

front of the nucleus.



fibrinogen stripes (green). Frames were collected in every 5 minutes. Display rate: 10 frames/second. Video 1 is related to Fig. 1.

**Legend for Video 2.** Reversive nuclear motion in a single C6 cell on a 20  $\mu$ m wide Alexa488-labeled cell adhesive fibronectin-fibrinogen stripe. Frame size: 270x60  $\mu$ m<sup>2</sup>. Frames were collected in every 5 minutes. Display rate: 8 frames/second. Video 2 is related to Fig. 2.

**Legend for Video 3.** The effect of 30 nM taxol administered 16 h after the beginning of the movie on auto-reverse nuclear migration in C6 cells cultured on 20  $\mu$ m wide stripes. Frames were collected in every 5 minutes. Display rate: 8 frames/second.

**Legend for Video 4.** The effect of 20 nM vinblastine administered 9 h after the beginning of the movie on auto-reverse nuclear migration in C6 cells cultured on 20  $\mu$ m wide stripes. Frames were collected in every 5 minutes. Display rate: 8 frames/second.

**Legend for Video 5.** The effect of 500 nM cytochalasin D administered 12 h after the beginning of the movie on autoreverse nuclear migration in C6 cells cultured on 20  $\mu$ m wide stripes. Frames were collected in every 5 minutes. Display rate: 10 frames/second.

	cell type	substrate	drug	day 1		day 2	
sample				velocity [μm/h]	n	velocity [μm/h]	n
1	C6	FN	-	$27 \pm 22$	871	$27 \pm 14$	757
2	C6	FN	-	$28 \pm 13$	728	n.a.	n.a.
3	C6	PLL	-	$23 \pm 13$	841	$28 \pm 14$	347
4	C6	PLL		n.a.	n.a.	$33 \pm 8$	965
5	C6	PLL		$25 \pm 5$	1065	n.a.	n.a.
6	C6	PLL		$21 \pm 11$	1123	$32 \pm 13$	431
7	PMF	PLL	-	$26 \pm 9$	488	$24 \pm 6$	1314
8	PMF	PLL		$15 \pm 3$	256	$24 \pm 16$	1051
9	C6	PLL	$100 \mu \text{M}$ AMP-PNP	$31 \pm 10$	844	$34 \pm 8$	463
10	C6	PLL	$100 \mu \text{M}$ AMP-PNP	$37 \pm 4$	476	$35 \pm 11$	374
11	C6	PLL	200nM citochalasin D	$10 \pm 5$	407	$12 \pm 5$	114
12	C6	PLL	500nM citochalasin D	$17 \pm 6$	666	$10 \pm 3$	956
13	C6	FN	$1 \mu$ M ML-7	$17\pm7$	879	$19 \pm 5$	674
14	C6	FN	30 nM taxol	$25 \pm 11$	372	$8\pm2$	390
15	C6	PLL	$5\mu\mathrm{M}$ vanadate	$30 \pm 9$	357	$31 \pm 11$	378
16	C6	PLL	20nM vinblastine	$34 \pm 0$	306	$3\pm0$	262

Table 1: Summary of experimental data. Population-averaged nuclear velocities were obtained from cells engaing in reversive nuclear motion. n denotes the number of positions used for calculationg the average velocities. PMF: primary mouse fibroblast; FN: Fibronectin-Fibrinogen; PLL: poly-l-lysine.